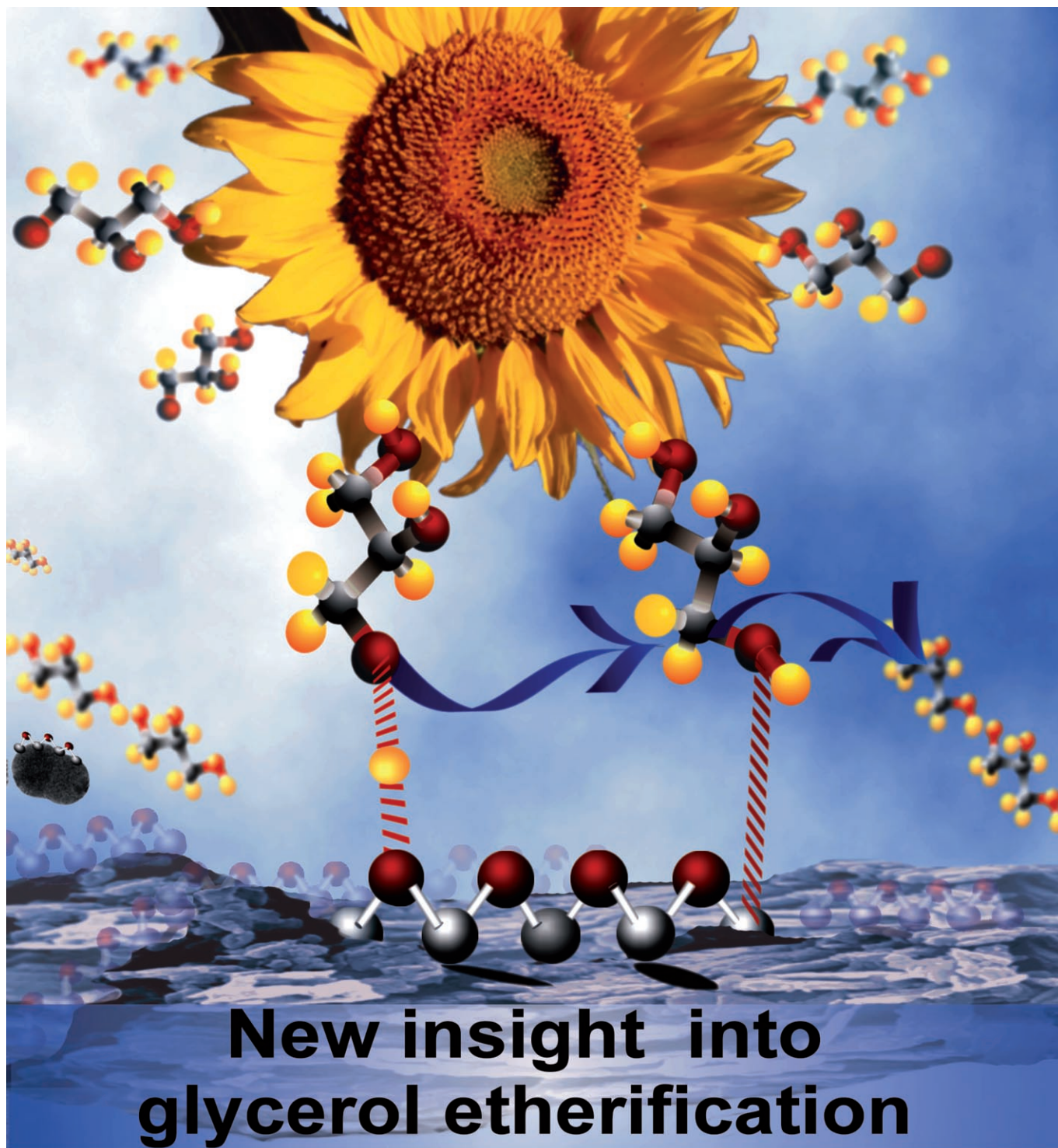# Glycerol Etherification over Highly Active CaO-Based Materials: New Mechanistic Aspects and Related Colloidal Particle Formation

Agnieszka M. Ruppert,[a] Johannes D. Meeldijk,[b] Bonny W. M. Kuipers,[c] Ben H. Erné,[c] and Bert M. Weckhuysen*[a]

New insight into glycerol etherification

Abstract: Glycerol is an attractive renewable building block for the synthesis of di- and triglycerols, which have numerous applications in the cosmetic and pharmaceutical industries. In this work, the selective etherification of glycerol to di- and triglycerol was studied in the presence of alkaline earth metal oxides and the data are compared with those obtained with Na_2CO_3 as a homogeneous catalyst. It was found that glycerol conversion increased with increasing catalyst basicity; that is, the conversion increases in the order: $MgO < CaO < SrO < BaO$. The best selectivity values for (di- + tri-) glycerol ($>90\%$ at 60% conversion) are obtained over CaO, SrO, and BaO. For these catalysts no substantial acrolein formation was observed. Furthermore, at the start of the reaction mainly linear diglycerol was produced, whereas at higher conversion degrees branched diglycerol started to form. In another series of experiments different types of CaO materials were prepared. It was found that these CaO-based materials not only differed in their surface area and number of basic sites, but also in their Lewis acid strength. Within this series the CaO material possessing the strongest Lewis acid sites had the highest catalytic activity, comparable to that of BaO, pointing towards the important role of Lewis acidity for this etherification reaction. Based on these observations a plausible alternative reaction scheme for glycerol etherification is presented, which considers the facilitation of the hydroxyl leaving process. Finally, the stability of the catalytic solids under study was investigated and it was found that colloidal CaO particles of about 50–100 nm can be spontaneously generated during reaction. Catalytic testing of these CaO colloids, after isolation from the reaction medium, revealed a very high etherification activity. Understanding the nature of these Ca-based colloids opens new opportunities for investigating supported colloidal particle catalysts to take advantage of both their hetero- and homogeneous nature.

Keywords: alkaline earth metals · biodiesel · calcium oxide · colloids · glycerol · heterogeneous catalysis

Introduction

Glycerol has recently attracted much attention in open and patent literature as a viable, highly functionalized building block for the synthesis of various intermediate compounds used in chemical industries.[1–6] Glycerol can be derived from the fermentation of glucose, from hydrogenolysis of sorbitol or as a waste product in the production of biodiesel from the transesterification of plant oils and animal fats.[1–6] Due to the growing biodiesel production, especially in Europe, the availability of glycerol has greatly increased. As a consequence, its price has significantly dropped to as low as $0.1\ \$kg^{-1}$ of crude glycerol, making it an even more attractive starting material for chemical production.[7] Several (potential) applications have been evaluated over the past years and some recent review papers are devoted to this emerging research topic.[8–12] Among its applications, glycerol can be a starting reagent for the synthesis of di- and triglycerol, which have numerous applications, for example, in cosmetic and pharmaceutical industries. Their market is predicted to develop significantly in the near future. Conventional methods for polyglycerol synthesis remain rather difficult, since this reaction requires drastic conditions; that is, a high reaction temperature and a caustic environment.[13] The use of for example, Na_2CO_3 as a homogeneous catalyst gives a high conversion, but relatively low selectivity, and several filtration, purification, and neutralization steps are required to recover almost pure diglycerol afterwards.[14] This procedure leaves large amounts of basic aqueous waste, which is not environmentally friendly.[15] Therefore, there is a need to search for highly active, selective, and stable heterogeneous catalysts for this important catalytic process.

Some research has already been pursued in this field, mainly covered in patents, but also reported in the open literature. More specifically, the group of Clacens have evaluated both microporous and mesoporous crystalline materials in the absence and presence of various promoter elements and prepared in different manners.[13–16] In the case of microporous solids, Cs-exchanged X zeolites were found to be active and selective catalysts with a glycerol conversion and (di- and tri-) glycerol selectivity of 79 and 95%, respectively, at a reaction temperature of 260°C. Instead, Cs-exchanged ZSM-5 materials showed to be much less active. The most promising results were obtained with mesoporous MCM-41 catalysts loaded with Cs, which have a (di- and tri-) glycerol selectivity of 97% at a conversion level of 80%. As far as catalyst leaching and stability are concerned it was noted by Clacens and co-workers that the best results were obtained with grafted solids that retain their structure and specific area, properties which were not observed for their impreg-

[a] Dr. A. M. Ruppert, Prof. Dr. B. M. Weckhuysen
Inorganic Chemistry and Catalysis group
Department of Chemistry, Faculty of Science
Utrecht University, Sorbonnelaan 16
3584 CA Utrecht (The Netherlands)
Fax: (+31)30-251-1027
E-mail: b.m.weckhuysen@uu.nl

[b] J. D. Meeldijk
Electron Microscopy Utrecht, Department of Biology
Faculty of Science, Utrecht University
Padualaan 8, 3584 CH Utrecht (The Netherlands)

[c] Dr. B. W. M. Kuipers, Dr. B. H. Erné
Van't Hoff Laboratory for Physical and Colloid Chemistry
Department of Chemistry, Faculty of Science
Utrecht University, Padualaan 8, 3584 CH Utrecht (The Netherlands)

nated mesoporous catalysts. Finally, in the case of Mg- and La-containing mesoporous catalysts it was found that the double dehydration to acrolein as catalyzed by acid sites is significant, excluding them as potential selective catalysts for the synthesis of di- and triglycerol.

In the current work, we have studied the glycerol etherification reaction over alkaline earth metal oxides (BaO, SrO, CaO, and MgO) as potential heterogeneous catalysts with high activity. More specifically, we concentrated on exploring the catalytic potential of different CaO materials as an example of an environmentally friendly and, according to some literature examples, one of the most stable materials among alkaline earth oxides.[17] To investigate various factors that could influence the activity and selectivity of these catalyst systems, we have focused our study on the following three areas:

1) Evaluating the influence of catalyst basicity on the etherification of glycerol and comparing the data with those obtained for the industrially employed homogeneous Na_2CO_3 catalyst. Special attention is directed towards the product distribution, including the formation of linear and branched oligomers of glycerol.
2) Exploring the catalytic properties of CaO materials synthesized in different ways and linking these catalytic data to their acid–base properties. For this purpose, basicity tests were performed with suitable Hammett indicators in combination with UV/Vis/NIR spectroscopy, whereas Lewis acidity was evaluated with IR spectroscopy in combination with pyridine as probe molecule.
3) Assessing the heterogeneous nature of the active CaO materials by studying the potential problems of catalyst leaching and colloidal particle formation during catalytic reaction. For this purpose, static light scattering (SLS) as well as cryo-TEM experiments were performed.

It will be shown that CaO-based materials containing the right balance of Lewis acid and basic sites possess very high activity in the selective etherification of glycerol towards di- and triglycerol. This activity may surpass even that of the most basic alkaline oxide BaO. Based on these results a tentative mechanism is postulated that involves not only basic sites, but also Lewis acid sites. In addition, it was observed that highly reactive CaO-based colloids can be formed in situ during catalysis, which opens new opportunities for investigations of supported colloidal particle catalysts to take advantage of both their hetero- and homogeneous nature.

Results and Discussion

Effect of catalyst basicity on the etherification of glycerol: One of the goals of this research work was to explore different heterogeneous catalysts for the selective synthesis of di- and triglycerol, avoiding the formation of higher oligomers of glycerol as well as acrolein as byproducts. Formation of this last product is known to be catalyzed by solid acids,[18–20]

therefore the choice for basic oxide materials, such as alkaline earth metal oxides, is clear. Indeed, parallel experiments in our laboratory, not shown for sake of brevity, indicated that zeolite-based materials, as well as lanthanide and lanthanide oxide chloride materials, lead to the formation of substantial amounts of acrolein. On the other hand, acrolein can also be formed by the thermal decomposition of glycerol and therefore it is not possible to completely avoid its formation. However, by decreasing the reaction temperature to 220 °C we have managed to slow down the decomposition reaction of glycerol so that acrolein formation in our experiments was never higher than 5 wt % after 20 h of the reaction. We note here that our reaction temperature is 40 °C lower than the one used in the work of Clacens and co-workers.[13] To allow comparisons between our study and their research we have included Na_2CO_3 as a reference homogeneous catalyst.

Figure 1 (top) shows the glycerol conversion for low surface area ($< 5\ m^2 g^{-1}$) MgO, CaO, SrO, and BaO materials as a function of reaction time. The relative catalytic activities
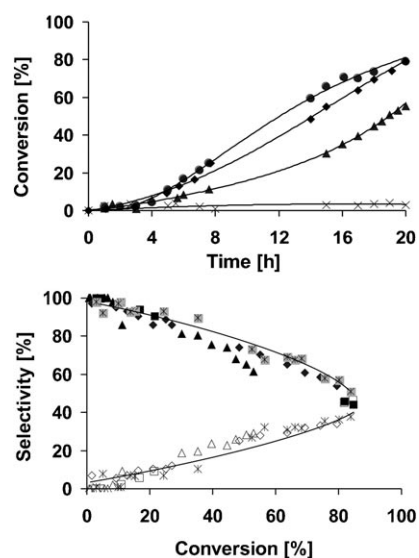
Figure 1. Top: Catalytic conversion (%) of glycerol at a temperature of 220 °C as a function of reaction time for BaO (●), SrO (♦), CaO-A (▲), and MgO (×); Bottom: Selectivity patterns (%) towards diglycerol for BaO (♦), SrO (■), CaO-A (▲), and Na_2CO_3 (■) and triglycerol for BaO (◇), SrO (□), CaO-A (△), and Na_2CO_3 (×) as a function of glycerol conversion (%).

of the alkaline earth metal oxides, summarized in Table 1, as the amount glycerol converted per gram of catalyst after 20 h of reaction, indicate the following reactivity order: BaO ≈ SrO > CaO ≫ MgO. This order is in accordance with their basicity;[21] that is, BaO > SrO > CaO > MgO and this observation was confirmed by performing independent basic strength measurements making use of Hammett indicators of the alkaline earth metal oxide materials under study. The results of this approach are included in Table 1. It is remarkable that MgO showed almost no conversion in the etherifi-

Table 1. Catalytic activity of MgO, CaO, SrO, and BaO, expressed as the amount of glycerol converted per gram of catalyst after 20 h at a temperature of 220 °C, as well as the overall surface basicity of the alkaline earth metal oxides as examined with the Hammett indicator method. In addition, we have measured the Lewis acidity for the different materials making use of pyridine as probe molecule in conjunction with IR spectroscopy. For comparison, the homogeneous catalyst Na_2CO_3 is included. (n.a.-not applicable; n.o.-not observed).

| Catalyst	$\Delta\nu_{8a}$ [cm^{-1}]	Moles of glycerol[a]	Basicity
Na_2CO_3	n.a.	0.43	$(13.4 > pK_{BH+} > 11)$
BaO	n.o.	0.41	$(17.2 > pK_{BH+} > 15)$
SrO	n.o.	0.41	$(17.2 > pK_{BH+} > 15)$
CaO	14	0.29	$(15 > pK_{BH+} > 13.4)$
MgO	22	0.04	$(8.2 > pK_{BH+} > 6.8)$

[a] Moles of glycerol converted per gram of catalyst after 20 h of reaction.

cation of glycerol and a conversion level well below 10 % was achieved after 20 h. In the case of BaO and SrO the conversion was initially low, but gradually reached a final value of about 80 %. The catalytic activity of CaO was slightly lower in comparison with BaO and SrO, but it was still possible to reach a conversion of about 60 % after 20 h of reaction.

In terms of conversion plotted against time, for all heterogeneous materials an activation period was observed in the first 3 h of reaction with very low glycerol conversion levels (Figure 1, top). To evaluate the selectivity behavior of MgO, CaO, SrO, BaO, and Na_2CO_3 we have plotted the selectivities towards diglycerol and triglycerol as a function of glycerol conversion (Figure 1, bottom). It is evident that no real differences in selectivity behavior are noted between the different catalyst materials under study and that with increasing glycerol conversion the selectivity towards triglycerol gradually increases at the expense of the selectivity towards diglycerol.

An additional selectivity feature that attracted our attention was the changing distribution of the formed diglycerol with reaction time. The possible isomeric diglycerol molecules can be linear, branched, and cyclic, as depicted here.

We observed that during glycerol etherification mainly linear and branched isomers are formed, regardless of the

cyclic diglycerols

branched diglycerols
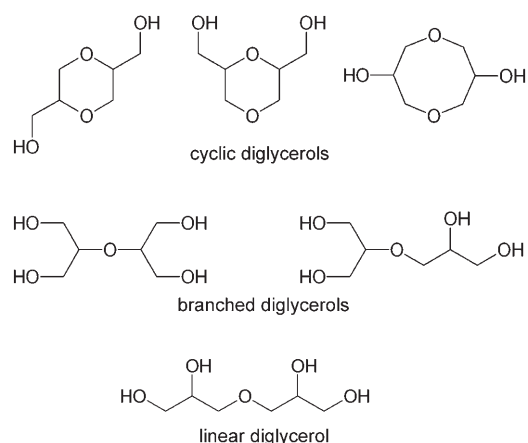
linear diglycerol

catalyst material used. At the beginning of reaction linear diglycerol is formed as the major product, while the branched form starts to dominate at higher glycerol conversion. We presume that the linear form of diglycerol is formed first as the kinetic product and then it partly equilibrates into branched diglycerol, which is favored thermodynamically. Another explanation could be that the formed linear diglycerol reacts faster than its branched isomers to form higher oligomers of glycerol. Both explanations, however, do not exclude each other.

It is known that the etherification of glycerol can be catalyzed by both acidic and basic catalysts. In the presence of an acidic catalyst a hydroxy group of glycerol is protonated, which renders it a good leaving group. It is followed by the nucleophilic attack of a hydroxy group of another glycerol molecule, accompanied by the leaving of the water molecule. Finally, the formed ether is deprotonated, yielding the respective di- or polyglycerol. This reaction can follow the S_N1 (via a carbocation) or S_N2 pathway (through a direct nucleophilic attack). As mentioned above, in the acidic conditions also a side reaction may take place. The protonated hydroxy group can leave as a water molecule. The formed carbocation releases a proton, yielding the hydroxyaldehyde. In a similar way, double elimination of water from glycerol leads to the formation of acrolein. To the best of our knowledge, only one explanation has been reported for the base-catalyzed glycerol etherification mechanism[22] involving the deprotonation of a hydroxy group and the attack of the formed alkoxy anion on the carbon of another glycerol molecule. This is shown in Scheme 1. However, the authors presume that a hydroxy anion leaves on its own, which would be quite difficult due to its strong nucleophilicity. Furthermore, no explanation has been put forward for how the hydroxyl group is rendered a sufficiently good leaving group. We can only presume that the reaction might be facilitated by very high temperature. Besides that, it would be most plausible that other surface groups of the catalytic solid may participate in the reaction mechanism, as will be discussed below.

Effect of catalyst Lewis acidity on the glycerol etherification: As was presented so far, the catalytic activity of the different alkaline earth metal oxides for the etherification of glycerol increases with catalyst basicity.

However, taking into account other aspects, such as toxicity in case of potential catalyst leaching, CaO among the alkaline earth metal oxides has the most potential to become a suitable heterogeneous catalyst for commercial applications, provided that its activity can be further improved and it is sufficiently stable during reaction. To achieve this goal we have synthesized various CaO catalytic materials differing in their physicochemical properties, further labeled as CaO-A, CaO-B, and CaO-C. These materials were tested in the etherification of glycerol at 220 °C and the catalytic activity data are shown in Figure 2. The amounts of glycerol converted per gram of catalyst after 20 h of reaction for the Ca-based catalysts under study are summarized in Table 2.
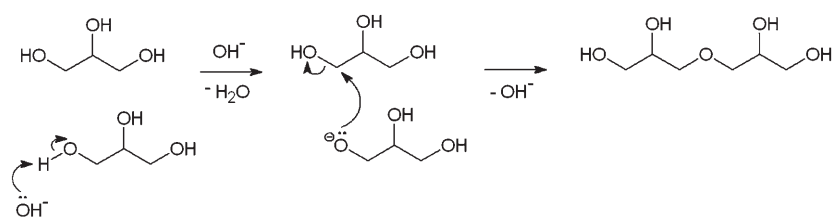
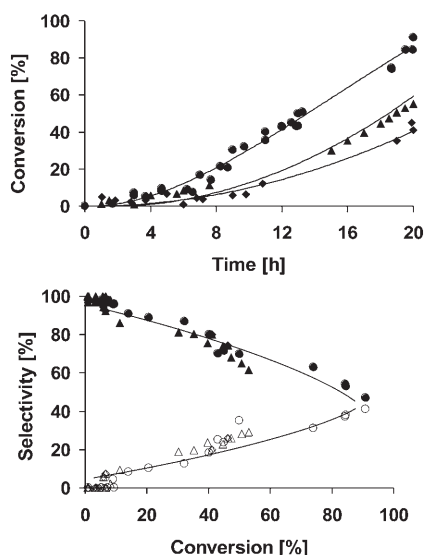Scheme 1. Reaction scheme for the base-catalyzed glycerol etherification.[21]

Figure 2. Top: Catalytic conversion (%) of glycerol at a temperature of 220 °C as a function of reaction time for CaO-A (♦), CaO-B (▲), and CaO-C (●). Bottom: Selectivity patterns (%) towards diglycerol for CaO-A (♦), CaO-B (▲), and CaO-C (●) and triglycerol for CaO-A (◇), CaO-B (△), and CaO-C (○) as a function of glycerol conversion (%).

Table 2. Catalytic activity of CaO-A, CaO-B, and CaO-C expressed as the amount of glycerol converted per gram of catalyst after 20 h at a temperature of 220 °C, together with some physicochemical properties of the catalysts.

Catalyst	Glycerol converted[a]	Basicity	BET [$m^2 g^{-1}$]	$\Delta \nu_{8a}$ [cm^{-1}]	Ca[%][b]
CaO-A	0.29	$15 > pK_{BH+} > 13.4$	2	14	3.0
CaO-B	0.22	$15 > pK_{BH+} > 13.4$	76	14	4.1
CaO-C	0.52	$15 > pK_{BH+} > 13.4$	54	18	6.0

[a] Moles of glycerol converted per gram of catalyst after 20 h of reaction. [b] % Ca in liquid phase (ICP).

It is evident that after an induction or activation period the glycerol conversion gradually increased with increasing reaction time. The glycerol conversion after 20 h of reaction increased in the order: CaO-B < CaO-A < CaO-C. Furthermore, it was found that the CaO-C material can reach a comparable to higher final glycerol conversion level after 20 h of reaction as compared to BaO and Na$_2$CO$_3$ (Table 1 vs. Table 2), but still keeping a high selectivity towards diglycerol. Figure 2 (bottom) compares the selectivity patterns towards di- and triglycerol as a function of the glycerol con-

version level for CaO-A, CaO-B, and CaO-C. Clearly, a similar behavior is noted as for the other alkaline earth metal oxide catalysts under study and with increasing glycerol conversion the selectivity towards triglycerol gradually increases. In a similar fashion, the relative ratio of linear over branched diglycerol changes with reaction time.

One of the questions that we have to address is what is responsible for the catalytic differences between CaO-A, CaO-B, and CaO-C. For this purpose, we have characterized the catalyst materials with different methods, which shed insight in their acid–base properties. First of all, we have evaluated the basic strength of the three CaO materials, as measured by the Hammett indicators method, taking Clayton Yellow as a suitable indicator since this molecule showed to be able to react with CaO-B and CaO-C, but only to a minor extent with CaO-A. The basic character of CaO material is caused by the presence of coordinative unsaturated oxide (Ca—O^{2-}) and hydroxide Ca—OH$^-$ sites. The related microphotographs of CaO-A, CaO-B, and CaO-C catalyst materials brought in contact with Clayton Yellow are shown in Figure 3. It can be noted that there are differences in the color intensities in the changed form of indicator, which
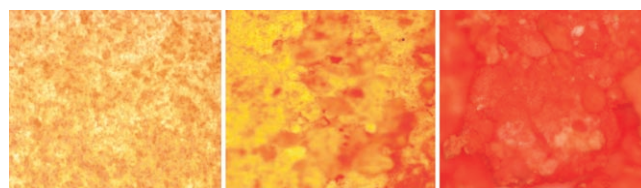

Figure 3. Color microphotographs of CaO-A (left), CaO-B (middle), and CaO-C (right) catalyst materials brought in contact with Clayton Yellow as Hammett indicator (yellow-orange = unreacted form; red = reacted form, zoom 200 ×).

should be related to the amount of surface basic sites. It is important to mention here that the surface areas of the three CaO materials are also different and follow the order: CaO-A ≪ CaO-C < CaO-B. However, although CaO-B has a larger surface area than CaO-C, it is not so reactive towards Clayton Yellow. In other words, the number of strong basic sites should be larger in CaO-C than in CaO-B. In line with this reasoning, the CaO-A material is the least basic catalyst material, since it remained yellow-orange and therefore only a minor fraction of the basic sites are able to convert the Clayton Yellow indicator towards its basic form. Based on these results one can conclude that basic strength and number of basic sites cannot explain the catalytic differences noted between especially CaO-B and CaO-C.

However, other surface properties, such as Lewis acidity, may also play a role in the etherification of glycerol. It is

known from literature that CaO possesses some Lewis acidity associated with coordinative unsaturated Ca atoms.[23] Inspired by this we have performed pyridine adsorption on the CaO-A, CaO-B, and CaO-C samples to determine their Lewis acidity. For this purpose, we have measured the blue shift of the C=C stretching band of adsorbed pyridine as compared to the value of 1580 cm^{-1} for gas-phase pyridine, further denoted as $\Delta\nu_{8a}$. It is known that the blue shift increases with increasing strength of the Lewis acid sites involved in the pyridine interaction.[24] The results are summarized in Table 2 and the most active catalyst, CaO-C, proved to possess the strongest Lewis acidity, as evidenced by its $\Delta\nu_{8a}$ value of 18 cm^{-1}. Catalyst materials CaO-A and CaO-B are characterized by a $\Delta\nu_{8a}$ value of 14 cm^{-1}. For comparison, we also measured the $\Delta\nu_{8a}$ values for BaO, SrO, and MgO and these values are included in Table 1. We have found that BaO and SrO did not show any substantial Lewis acidity, whereas MgO possesses strong Lewis acid sites. Although Lewis acidity is certainly not the sole parameter that may influence the catalytic properties of CaO-A, CaO-B, and CaO-C, the Lewis acidity measurements indicate its potential role in the glycerol etherification mechanism. Indeed, the mechanism of a base-catalyzed etherification, as outlined in Scheme 1, is difficult to explain without the involvement of Lewis acid sites by the activation of a hydroxy group as a leaving group. Therefore we tentatively postulate the role of coordinative unsaturated surface metal ions, which facilitate the hydroxyl leaving process in the glycerol etherification reaction as depicted in Scheme 2.
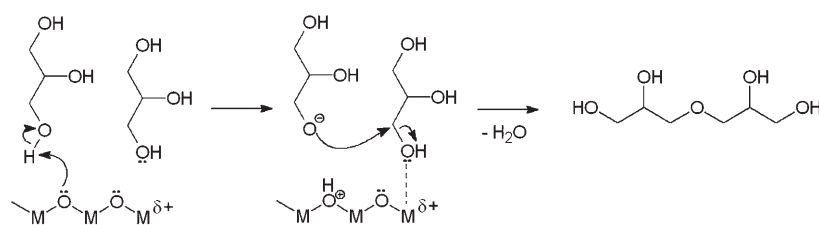
Scheme 2. Potential reaction scheme for the base-catalyzed glycerol etherification involving Lewis acidity.

Examples of such dual mechanism involving both basic and Lewis acid active sites has also been reported for other heterogeneous catalytic reactions, for example, the destructive adsorption of chlorinated hydrocarbons on lanthanide oxide and oxide chloride materials.[25,26]

Catalyst stability during glycerol etherification and related colloidal particle formation: As discussed above the etherification of glycerol to di- and triglycerol can be catalyzed by heterogeneous basic oxides, such as CaO, and high conversion degrees are obtained if the right combination of basicity and Lewis acidity is present at the catalyst surface. However, in many of our catalytic experiments an induction or activation period was observed, as shown in Figure 2 (top), suggesting that catalyst leaching phenomena could have taken place. Furthermore, in specific cases a milky reaction

mixture was observed. Therefore, besides the CaO solid, the active species involved might be the Ca ions, most probably in the form of calcium diglyceroxide.[27] Another, even more plausible assumption for this activation period is that CaO catalyst particles are partially hydroxylated due to the formation of water formed during the glycerol etherification reaction, which is followed by the fragmentation of the catalyst material and the formation of Ca(OH)$_2$ colloids. Neither of these explanations excludes the other.

To verify this hypothesis we have taken samples from the reactor after different reaction times. These reaction mixtures were analyzed for the amount of CaO going into the liquid phase (dissolved or as colloidal particles) by using inductively coupled plasma analysis (ICP) after centrifugation. The ICP results are shown in Table 2 for samples CaO-A, CaO-B, and CaO-C after 2 h of the reaction. It can be seen that about 3–6% of Ca from the original CaO catalyst material can be found in the liquid phase already after 2 h of reaction and these amounts gradually increased with reaction time (Figure 4). At the earliest stages of the reaction, the highest amount is observed for the most active CaO-C sample and by comparing Figures 2 (top) and 4 it is clear that the activation course of the different catalyst materials goes hand in hand with increasing amounts of CaO material going into the reaction solution. It is important to stress at this point that the ICP analysis does not allow us to distinguish between the formation of Ca(OH)$_2$ complexes and Ca(OH)$_2$ colloids in the reaction mixture and other techniques had to be called in to substantiate these findings further.

Two techniques may prove whether indeed Ca(OH)$_2$ colloids are formed during the glycerol etherification over CaO materials: cryo-TEM and static light scattering (SLS). Figure 5 summarizes the SLS measurements performed on sample CaO-A for increasing reaction time. It is clear that the scattering intensity of the reaction mixture is gradually increasing with reaction time and therefore with growing amount of CaO found in the solution. Furthermore, the formation of colloidal Ca(OH)$_2$
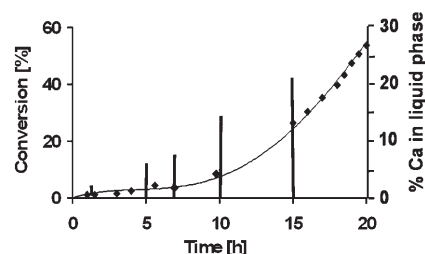

Figure 4. Conversion (◆) (left-hand scale) and fraction of CaO catalyst material going into solution (%) (bar graph) (right-hand scale) measured with ICP as a function of reaction time for CaO-A.
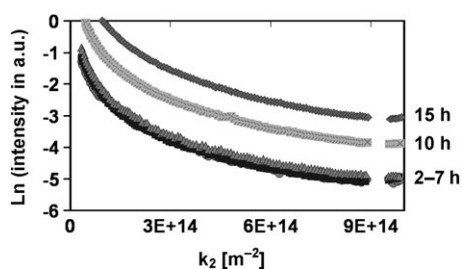
Figure 5. Static light scattering results for CaO-A for different reaction times.

particles was confirmed already after 2 h of reaction. Cryo-TEM of vitrified reaction mixture, on the other hand, provided further insight into the size and shape of the colloidal Ca(OH)$_2$ particles formed and a representative set of TEM pictures are shown in Figure 6. The colloidal particles are spherical and can be present as isolated particles or aggregates in different forms. By performing a systematic analysis of the size and number of the colloidal particles formed as measured with TEM it was possible to determine the average particle sizes of the colloidal particles formed during glycerol etherification from samples CaO-A, CaO-B, and CaO-C. This is illustrated in Figure 7. A high polydispersity is observed for all samples under study and the average particle size (d_s for the colloidal particles originating from CaO-A and CaO-B is about 65 nm, whereas those formed from sample CaO-C are slightly larger (93 nm) in size.

In the case of sample CaO-A the colloidal particle distribution seems to be bimodal, although, the statistical analysis
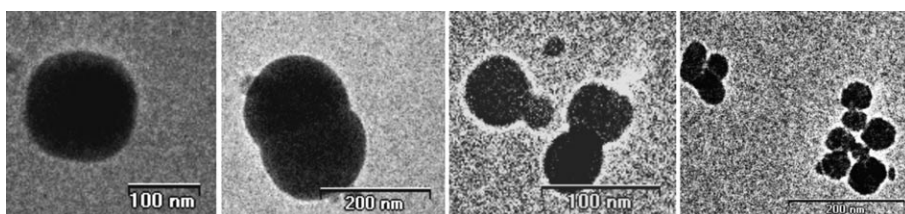

Figure 6. Typical cryo-TEM micrographs of colloidal particles formed during the glycerol etherification over CaO-C (left pair of images), and CaO-B (right pair of images).
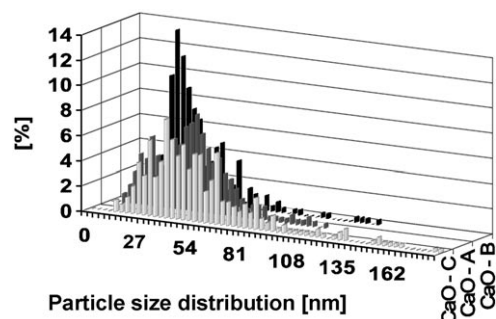

Figure 7. Colloidal particle size distribution for CaO-A, CaO-B and CaO-C after 2 h of glycerol etherification as determined from a statistical analysis of the cryo-TEM micrographs. Calculated d_s value ($\Sigma n_i \cdot d_i^3 / \Sigma n_i \cdot d_i^2$) CaO-B (64 nm); CaO-A (66 nm); CaO-C (93 nm).

performed could be affected by the presence of aggregates of Ca(OH)$_2$ colloidal particles.

Remarkably for colloidal CaO, a very high glycerol conversion of 1.45 mol glycerol per gram catalyst after 20 h of reaction was obtained and this value is higher than the conversion value of 0.29 mol of glycerol obtained for the CaO-A material, in which the colloidal Ca(OH)$_2$ particles originate from. Similar observations were made for the CaO-B and CaO-C samples. It is important to note that basicity measurements making use of the Hammett indicators allowed us to determine the overall basicity of these colloids, which was higher than that of CaO-A. Unfortunately, it was impossible to perform similar experiments to measure the Lewis acidity strength of these colloids samples.

Conclusion

Different alkaline earth metal oxides (MgO, CaO, SrO, and BaO) were tested as potential heterogeneous catalysts for the etherification of glycerol towards di- and triglycerol and the results were compared with those obtained with Na$_2$CO$_3$ as a homogeneous catalyst. The following conclusions can be drawn from this study:

1) Glycerol etherification over alkaline earth metal oxide based catalysts is controlled by both their surface basicity and Lewis acidity. First of all, it was found that glycerol conversion increased with increasing catalyst basicity; that is, the conversion increases in the order: MgO < CaO < SrO < BaO. In addition, testing of various CaO-based materials showed that the surface area and the strength of both basic and Lewis acid sites matter and the catalyst material with the right balance of basicity and Lewis acidity possesses the highest glycerol etherification activity. By doing so a CaO-based catalyst material can be prepared with an activity comparable with that of the most basic alkaline earth metal oxide; that is, BaO. Based on these observations a plausible alternative reaction scheme involving both basic and Lewis acid sites for glycerol etherification is presented.

2) Glycerol etherification at temperatures as high as 220°C in the absence of a solvent represents rather harsh experimental conditions for a heterogeneous catalyst material. As a result, depending on the preparation and treatment of the catalyst the material can defragment and form colloidal particles during the course of the reaction. More specifically, it was found that colloidal CaO particles of about 50–100 nm are spontaneously generated during reaction and their amount gradually increases with increas-

ing reaction time. The glycerol conversion goes hand in hand with the amount of CaO colloidal particles in the reaction mixture. Catalytic testing of these CaO colloids, after isolation from the reaction medium, revealed a very high etherification activity, which may become of practical interest after finding a suitable way of immobilization since such supported colloidal systems would take advantage of both their hetero- and homogeneous nature.

Experimental Section

Catalyst preparation: Different alkaline earth metal oxides, that is, MgO, CaO, SrO, and BaO, were prepared by performing a high-temperature treatment of the corresponding metal nitrates ($Ca(NO_3)_2 \cdot 4H_2O$ (Sigma-Aldrich, 99%), $Mg(NO_3)_2 \cdot 4H_2O$ (Sigma-Aldrich, 99%), $Sr(NO_3)_2 \cdot 4H_2O$ (Sigma-Aldrich, 99%), and $Ba(NO_3)_2 \cdot 4H_2O$ (Sigma-Aldrich, 99%) in air in a porcelain crucible in a static manner. In all cases the respective nitrate (10 g) was heated to 700°C for 2 h with a heating rate of 10°Cmin^{-1}. In addition, two other CaO materials were synthesized, which are further denoted as CaO-B and CaO-C. The original CaO from the nitrate salt is also labeled for clarity as CaO-A. The CaO-B sample was made starting from commercial CaO (J.T. Backer, 96%) by heating the solid in the presence of distilled water at 80°C for 2 h under continuous stirring, followed by drying in a furnace at 120°C in a static manner overnight. The material was then activated under dynamic vacuum (10^{-3} Torr) at different temperatures: in the first step it was heated to 350°C with a heating rate of 0.5°Cmin^{-1}, followed by maintaining the temperature at 350°C for 1 h; and in the second step, further heating to 400°C or 500°C at a rate of 1°Cmin^{-1} and maintaining the temperature for 1 h. This activation treatment was done in a Schlenk tube, which was placed in a furnace.[28] The CaO-C sample was prepared from $Ca(OH)_2$ in the following manner. First, a solution of calcium methoxide was prepared by dissolving metallic Ca (16.8 g; Acros Organics, 99%) in dry methanol (800 mL; Biosolve, 99.9%). The mixture was stirred for 16 h under a flow of Ar to prevent calcium methoxide from reacting with atmospheric moisture. The following reaction [Eq. (1)] takes place during this process .

$$Ca + 2CH_3OH \rightarrow Ca(OCH_3)_2 + H_2 \qquad (1)$$
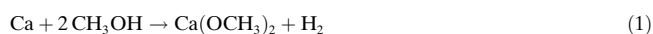
Then the solution of $Ca(OCH_3)_2$ in methanol (150 mL) was stirred in a beaker with toluene (450 mL) (Acros Organics, 99.99%). Calcium methoxide in this mixture was immediately hydrolyzed by dropwise addition of de-ionized water (8 mL) at room temperature [Eq. (2)].

$$Ca(OCH_3)_2 + 2H_2O \rightarrow Ca(OH)_2 + 2CH_3OH \qquad (2)$$
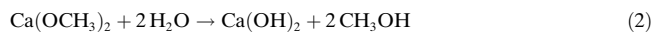
The reaction mixture was then transferred into an autoclave and flushed with Ar for 10 min. The autoclave was loaded with Ar to the pressure of 12 bar and heated to 245°C with a temperature gradient of 10°Cmin^{-1}. The final pressure in the autoclave was 39 bar and the temperature of 245°C was maintained for 15 min. After synthesis, the autoclave was vented, flushed with Ar for 10 min to remove the remaining organic solvents and allowed to cool down to room temperature. In the final step the obtained calcium hydroxide was thermally converted to CaO by performing the activation treatment under dynamic vacuum (10^{-3} Torr). For this purpose, $Ca(OH)_2$ was placed in a Schlenk tube, outgassed for 20 min and heated according to the following treatment: 25–350°C at a rate of 0.5°Cmin^{-1} and maintaining the temperature of 350°C for 1 h; followed by further heating to 400°C with a rate of 1°Cmin^{-1} and maintaining this temperature for 1 h. Sodium carbonate (Acros Organics, an-hydrous, pure), was used as delivered as reference homogeneous catalyst. In view of the applied synthesis procedure we may not exclude the presence of surface impurities, such as Fe ions (from the autoclave).

Catalyst characterization: Surface areas of all catalyst materials were determined by N_2 sorption measurements at liquid N_2 temperature with a Micromeritics Tristar 3000 apparatus. The Lewis acidity of the catalyst materials were determined by infrared spectroscopy (IR) making use of pyridine as probe molecule. All IR spectra were measured using a Perkin–Elmer FT-IR 2000 spectrometer. The catalyst materials were pressed into self-supporting wafers and activated at 450°C for 1 h under vacuum (0.075 Torr). A quartz cell was used at room temperature for the IR measurements. IR studies of the ν(C=C) ring vibrations, especially in the 1400–1700 cm^{-1} region, are considered as a general method to determine the strength of the Lewis acid sites of solid catalyst materials. Pyridine (Acros Organics, 99%+) adsorption, followed by evacuation, was carried out at room temperature, at a pressure of 11.2 Torr for 1 min. Desorption of pyridine was performed at room temperature at a pressure of 0.075 Torr for 1 h. Examination of the so-called ν_{8a} vibration of adsorbed pyridine, which is located at around 1580 cm^{-1}, is a measure of the Lewis acidity of a catalytic solid and an increasing blue shift from the ν_{8a} of liquid pyridine (1600 cm^{-1}) points towards an increasing Lewis acidity (further denoted as $\Delta\nu_{8a}$).[24] The basicity of the different catalyst materials were determined by the use of Hammett indicators. Their color change by interaction with the catalyst materials was evaluated with an UV/Vis/NIR Cary 500 Varian spectrometer in diffuse reflectance mode. For this purpose, neutral red (Acros Organics, certified), phenolphthalein (Aldrich, ethanol/water 50%), nile blue (Acros Organics, pure), tropaeolin-o (Acros Organics, pure), Clayton yellow (Acros Organics, certified), 2,4-dinitroaniline (Acros Organics, 99%), 4-chloro-2-nitroaniline (Aldrich, 99%) and p-dinitroaniline (Acros Organics, certified) were used. Their pK values are summarized in Table 1. The Hammett indicator tests were performed on fresh materials, which were stored under N_2. The catalyst sample (0.25 mg) was shaken with solution of the indicator in methanol (2 mL; Biosolve, 99.9%). A color change from the neutral to the deprotonated form of the indicator was observed. The base strength of the catalyst material, further denoted as pK_{BH+}, was defined as a value between the weakest indicato that changes the color and the strongest indicator that gives no color change. After that the solvent was evaporated and the color change of the remaining solid was analyzed by UV/Vis/NIR spectroscopy. Perkin–Elmer Optima-3000 apparatus was used to determine the chemical composition of the samples by inductively coupled plasma analysis (ICP). Each sample was taken from a separate experiment: after the given reaction time the experiment was stopped, the reaction mixture was centrifuged and a drop of the supernatant was diluted by a factor of 100 in 1 M HNO_3 prior to the ICP analysis. Colloid formation was studied by cryogenic transmission electron microscopy (cryo-TEM), because this technique allows the imaging of the colloids in situ and avoids drying effects that may change the TEM pictures. Prior to the experiments the samples containing colloids in glycerol as a solvent were diluted in ethylene glycol (Acros Organics 99%+). To decrease the viscosity of the mixture, the samples were preheated at 80°C. Vitrified films of Ca colloids were prepared in nitrogen atmosphere at 40°C on grids with carbon film in a so-called vitrification robot: the grid was immersed in the dispersion, blotted with filter paper (2×0.5 s) to remove the excess of solvent, and after 1 s it was vitrified by shooting it into liquid nitrogen. A transmission electron microscope (Tecnai 12, FEI) equipped with a cryo-holder (626 cryotransfer system, Gatan) was used at low-dose conditions to avoid melting the frozen dispersion film. Particle size distributions were calculated from TEM images, based on the sizes of 200 particles for each calculation. X-ray diffraction patterns of solid CaO materials were recorded on PANalytical X'Pert Pro system using Cu$_{K\alpha}$ radiation. Fresh samples were transferred to the instrument in airtight sample holders. The data were collected in the range $2\theta = 10$–90° with the step size of 0.027. Quantitative analysis was performed by comparison with the ICDD PDF 22000 database. Static light scattering (SLS) was done with an FICA 50 setup at a wavelength $\lambda_o = 546$ nm and a temperature of 25°C. The aggregated samples were diluted in ethylene glycol (Acros Organics 99%+) in order to decrease the viscosity. During preparation the mixtures were not protected from dust so the samples were

filtered prior to the measurements. Milliporous FP 1 μm filters were used. The scattered light intensity was measured as a function of the scattering angle (from 50 to 120).[29]

Catalytic testing: Glycerol etherification was carried out in a stirred batch reactor. Glycerol (50 g, Acros Organics, 99 % +) and the catalyst (1 g) were stirred at 220 °C for at least 20 h under Ar flow in a three-necked 250 mL flask equipped with a mechanical stirrer (500 rpm) and a Dean–Stark apparatus with a reflux condenser to collect water that was removed from the reaction mixture by the flow of gas. Some amounts of glycerol usually also condensed in the Dean–Stark apparatus. Additionally, acrolein was collected in a trap with dry ice, placed downstream from the condenser. The catalytic solids were fractionated before the reaction and the fraction between 850 and 500 mesh was used. In some cases the catalyst materials were placed in the reactor directly from the Schlenk tube without contact with air. Liquid samples were taken periodically and analyzed by HPLC (Shimadzu, (LC-20 AD) equipped with a Pathfinder column (4.6×250 mm) and RID (RID-10 A) detector and autosampler (SIL-20 A)). Water was used as an eluent. The selectivities towards different products were calculated as the molar ratio of the respective product to the sum of products formed.

Acknowledgements

[1] S. Demirel, K. Lehnert, M. Lucas, P. Claus, *Appl. Catal. B* **2007**, *70*, 637.

[2] R. S. Karinen, A. O. I. Krause, *Appl. Catal. A* **2006**, *306*, 128.

[3] K. Klepacova, D. Mravec, A. Kaszonyi, M. Bajus, *Appl. Catal. A* **2007**, *328*, 1.

[4] R. R. Soares, D. A. Simonetti, J. A. Dumesic, *Angew. Chem.* **2006**, *118*, 4086; *Angew. Chem. Int. Ed.* **2006**, *45*, 3982.

[5] S. H. Chai, H. P. Wang, Y. Liang, B. Q. Xu, *J. Catal.* **2007**, *250*, 342.

[6] D. A. Simonetti, J. Ross-Hansen, E. L. Kunkes, R. R. Soares, J. A. Dumesic, *Green Chem.* **2007**, *9*, 1073.

[7] Dave Nilles, *Biodiesel Magazine*, September **2006**.

[8] M. Pagliaro, R. Ciriminna, H. Kimura, M. Rossi, C. Della Pina, *Angew. Chem.* **2007**, *119*, 4516; *Angew. Chem. Int. Ed.* **2007**, *46*, 4434.

[9] J. N. Chheda, G. W. Huber, J. A. Dumesic, *Angew. Chem.* **2007**, *119*, 7298; *Angew. Chem. Int. Ed.* **2007**, *46*, 7164.

[10] P. Gallezot, *Catal. Today* **2007**, *121*, 76.

[11] G. W. Huber, S. Iborra, A. Corma, *Chem. Rev.* **2006**, *106*, 4044.

[12] A. Corma, S. Iborra, A. Velty, *Chem. Rev.* **2007**, *107*, 2411.

[13] J. Barrault, Y. Pouilloux, J.-M. Clacens, C. Vanhove, S. Bancquart, *Catal. Today* **2002**, *75*, 177.

[14] J. Barrault, J. M. Clacens, Y. Pouilloux, *Top. Catal.* **2004**, *27*, 137.

[15] J. M. Clacens, Y. Pouilloux J. Barrault, C. Linares, M. Goldwasser, *Stud. Surf. Sci. Catal.* **1998**, *118*, 895.

[16] J. M. Clacens, Y. Pouilloux, J. Barrault, *Appl. Catal. A* **2002**, *227*, 181.

[17] M. D. Z. P. M. López Granados, D. Martín Alonso, R. Mariscal, F. Cabello Galisteo, R. Moreno-Tost, J. Santamaría, J. L. G. Fierro, *Appl. Catal. B* **2007**, *73*, 317.

[18] M. Watanabe, T. Iida, Y. Aizawa, T. M. Aida, H. Inomata, *Bioresour. Technol.* **2007**, *98*, 1285.

[19] L. Ott, M. Bicker, H. Vogel, *Green Chem.* **2006**, *8*, 214.

[20] E. Tsukuda, S. Sato, R. Takahashi, T. Sodesawa, *Catal. Commun.* **2007**, *8*, 1349.

[21] H. Hattori, *Chem. Rev.* **1995**, *95*, 537.

[22] J. M. Clacens, Ph.D. Thesis, CNRS, Poitiers, 24 September **1999**.

[23] M. I. Zaki, H. Knözinger, B. Tesche, G. A. H. Mekhemer, *J. Colloid Interface Sci.* **2006**, *303*, 9.

[24] A. Travert, A. Vimont, A. Sahibed-Dine, M. Daturi, J.-C. Lavalley, *Appl. Catal. A* **2006**, *307*, 98.

[25] A. W. A. M. van der Heijden, V. Belierie, L. Espinosa Alonso, M. Daturi, O. V. Manoilova, B. M. Weckhuysen, *J. Phys. Chem. B* **2005**, *109*, 23993.

[26] A. W. A. M. van der Heijden, M. Garcia Ramos, B. M. Weckhuysen, *Chem. Eur. J.* **2007**, *13*, 9561.

[27] M Kouzu, T Kasuno, M. Tajika, S. Yamanaka, J. Hidaka, *Appl. Catal. A* **2008**, *334*, 357.

[28] O. Koper, Y-Xi. Li, K. J. Klabunde, *Chem. Mater.* **1993**, *5*, 500.

[29] S. Sacanna, A. P. Philipse, *Langmuir* **2006**, *22*, 10209.